A Unified Algorithm for Analysis and Simulation of Planar Four-Bar Motions Defined With R- and P-Joints

Xiangyun Li
Computational Design Kinematics Lab,
State University of New York at Stony Brook,
Stony Brook, NY 11794-2300

Xin Ge
Computational Design Kinematics Lab,
State University of New York at Stony Brook,
Stony Brook, NY 11794-2300

Anurag Purwar
Computational Design Kinematics Lab,
State University of New York at Stony Brook,
Stony Brook, NY 11794-2300

Q. J. Ge[1]
Computational Design Kinematics Lab,
State University of New York at Stony Brook,
Stony Brook, NY 11794-2300
e-mail: Qiaode.Ge@stonybrook.edu

This paper presents a single, unified, and efficient algorithm for animating the coupler motions of all four-bar mechanisms formed with revolute (R) and prismatic (P) joints. This is achieved without having to formulate and solve the loop closure equation for each type of four-bar linkages separately. Recently, we developed a unified algorithm for synthesizing various four-bar linkages by mapping planar displacements from Cartesian space to the image space using planar quaternions. Given a set of image points that represent planar displacements, the problem of synthesizing a planar four-bar linkage is reduced to finding a pencil of generalized manifolds (or G-manifolds) that best fit the image points in the least squares sense. In this paper, we show that the same unified formulation for linkage synthesis leads to a unified algorithm for linkage analysis and simulation as well. Both the unified synthesis and analysis algorithms have been implemented on Apple's iOS platform. [DOI: 10.1115/1.4029295]

1 Introduction

This paper revisits the well-studied problem of kinematic analysis of planar four-bar linkages formed with revolute (R) and prismatic (P) joints. The solutions to this problem are well known and are available in undergraduate textbooks on mechanism design and analysis. Typically, the problem is solved using the so-called vector loop closure equation which is formulated for a specific type of planar four-bar linkages such as planar RRRR or RRRP (slider–crank) mechanism [1,2]. Recently, we have developed a unified algorithm for simultaneous type and dimensional synthesis of planar four-bar linkages [3]. With the unified algorithm, we are able to determine the type of joints, either R or P, as well as the dimensions, simultaneously for finite position synthesis. In this paper, we seek to develop a unified algorithm for analysis and simulation of the resulting four-bar linkage, without having to know the mechanism type and then formulate the loop closure equation specifically for that particular type of mechanism. This has the potential to greatly improve efficiency of the software development and maintenance.

There have been significant academic and commercial research efforts in the development of software systems for the synthesis and animation of planar four-bar mechanisms such as SYMECH [4], WATT [5], SAM [6], and ADAMS [7]. But all these software products are restricted to four-bar linkages whose four joints are all revolute joints. In general, there are at most six possible types of four-bar mechanisms that can be constructed, which are RRRR, RRRP, RRPR, PRPR, PRRP, and RPPR. The advantage of the algorithm presented in Ref. [3] is that given a set of task positions, it can determine simultaneously the joint types (R or P) together with the link dimensions for motion generation. This algorithm has been implemented on iOS platform. Figure 1 shows the screenshot of the graphical user interface (GUI) of the synthesis program on iPad. The objective of the current paper is to develop a unified method for the analysis and animation of all six types of four-bar mechanisms.

We use a planar quaternion formulation to transform the task positions into points in the image space (see Refs. [8–10]). In this way, geometric constraints associated with planar dyads, such as circle or line constraints, are transformed into special quadric surfaces called constraint manifolds. In the process, we discovered a unified equation for the constraint manifolds for all planar dyads, namely, RR, PR, RP, and PP. Thus, regardless of the joint type, the image curve corresponding to a four-bar motion can be computed as intersection of two constraint manifolds with the same algebraic form.

Computing the intersection of two general quadrics is a classical problem in analytic geometry of three dimensions. This problem has been solved from the computer graphics perspective by Levin [11,12]. It is based on an analysis of a set formed by linear combinations of the two quadrics, called *a pencil of quadrics*. Building on Levin's pioneering work, Dupont et al. [13] presented the first practical and efficient algorithm for computing an exact parametric representation of the intersection for two quadric surfaces in three-dimensional space given by implicit equations with rational coefficients. In this paper, we apply the work of Levin

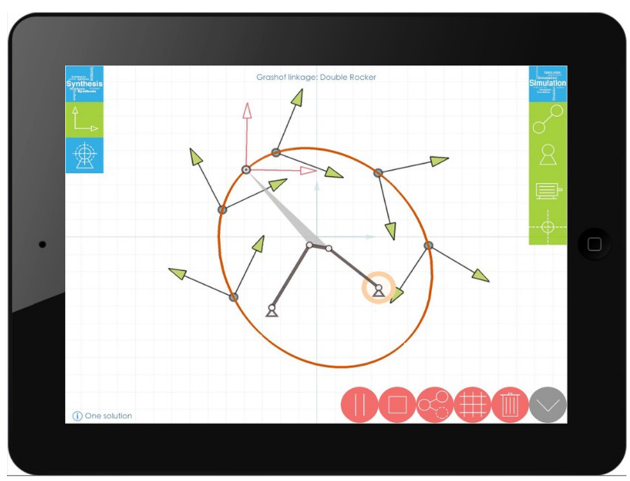

Fig. 1 The screen shot of GUI on iPad

[1]Corresponding author.

Manuscript received September 26, 2014; final manuscript received December 1, 2014; published online December 31, 2014. Assoc. Editor: Carl Nelson.

and Dupont to the development of a compact and efficient algorithm for computing the intersection of two G-manifolds and thus obtain a unified algorithm for the analysis and animation of all six types of planar four-bar linkages.

The organization of the paper is as follows. Section 2 reviews the conventional method for analyzing the coupler motion of a planar four-bar linkage. Section 3 presents the advocated algorithm for unifying the computation of the coupler motions generated by various four-bar linkages. Finally, we present six examples for each type of four-bar mechanism to demonstrate the efficacy of our approach.

2 Four-Bar Motion Analysis Based on the Loop-Closure Equation

In this section, we review the conventional approach to four-bar motion analysis using loop-closure equation. For simplicity, we use the RRRR-type as an example to outline the procedure.

Consider a planar 4R linkage shown in Fig. 2 with XOY being the fixed coordinate frame. The fixed pivot A_0 is located at point (x_0, y_0) with A_0B_0 being the ground link and A_0A the input link. Let l_i denote the length of the ith link and θ_1 be the angle of link A_0B_0 as measured from the X axis of the fixed frame. Let ϕ, λ, and ψ be the angles of link A_0A, AB, B_0B as measured from the ground link A_0B_0, respectively. A moving frame is attached to coupler link AB at P with β measured from AB to its x-axis. Polar coordinates (r, α) represent the position of P with respect to coupler AB. All the quantities except λ and ψ are known values after synthesis. When animating the 4R linkage, we rotate the input link A_0A with ϕ being known at a given moment. In order to calculate the position and orientation of moving frame relative to XOY at each value of ϕ, the key is to find the coupler angle λ.

Using loop-closure equation [2,14], the relationship between coupler angle λ and input link angle ϕ is given by

$$e^{i\lambda} = \frac{-B(\phi) \pm \sqrt{\Delta_1(\phi)\Delta_2(\phi)}}{2A(\phi)} \tag{1}$$

where

$$A(\phi) = l_{31}(l_{21}e^{-j\phi} - 1) \tag{2}$$

$$B(\phi) = 1 + l_{21}^2 + l_{31}^2 - l_{41}^2 - 2l_{21}\cos\phi \tag{3}$$

$$\Delta_1(\phi) = 1 + l_{21}^2 - (l_{31} + l_{41})^2 - 2l_{21}\cos\phi \tag{4}$$

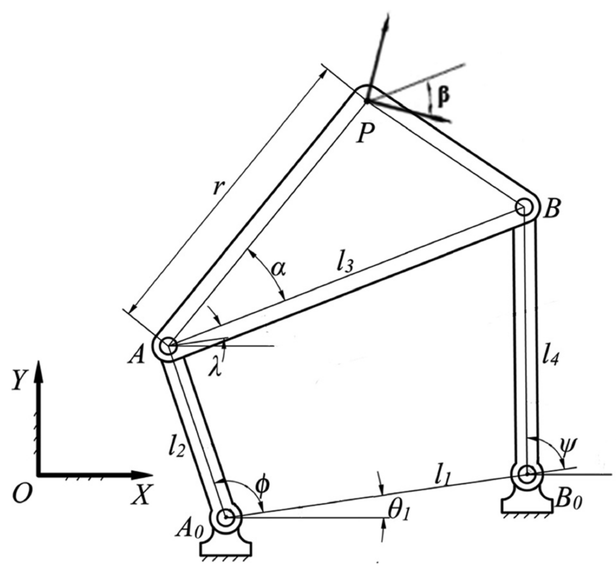

Fig. 2 A planar four-bar mechanism

$$\Delta_2(\phi) = 1 + l_{21}^2 - (l_{31} - l_{41})^2 - 2l_{21}\cos\phi \tag{5}$$

$$l_{21} = l_2/l_1, \quad l_{31} = l_3/l_1, \quad l_{41} = l_4/l_1 \tag{6}$$

and the sign $\pm$ corresponds to the two configurations of the four-bar linkage for the same input angle.

With λ being known, the position of moving frame, i.e., the position vector $\mathbf{P}$ of its origin P can be obtained by the following vector addition:

$$\mathbf{OP} = \mathbf{OA}_0 + \mathbf{A}_0\mathbf{A} + \mathbf{AP} \tag{7}$$

where

$$\mathbf{OA}_0 = [x_0, y_0] \tag{8}$$

$$\mathbf{A}_0\mathbf{A} = [l_2\cos(\phi + \theta_1), l_2\sin(\phi + \theta_1)] \tag{9}$$

$$\mathbf{AP} = [r\cos(\alpha + \lambda + \theta_1), r\sin(\alpha + \lambda + \theta_1)] \tag{10}$$

The orientation of moving frame is calculated as

$$\text{orientation} = \theta_1 + \lambda + \beta \tag{11}$$

Moreover, the position of moving pivot A and B can be easily obtained as follows:

$$\mathbf{OA} = \mathbf{OA}_0 + \mathbf{A}_0\mathbf{A} \tag{12}$$

$$\mathbf{OB} = \mathbf{OA}_0 + \mathbf{A}_0\mathbf{A} + \mathbf{AB} \tag{13}$$

where

$$\mathbf{AB} = [l_3\cos(\lambda + \theta_1), l_3\sin(\lambda + \theta_1)] \tag{14}$$

With the computed position and orientation of moving frame and coordinates of moving pivots, we are now able to draw the planar 4R mechanism with its coupler motion at each frame of animation. However, this loop-closure equation is only valid for planar RRRR linkage. A different type of planar four-bar linkage calls for a different loop closure equation. This means that one has to write six separate codes for all six types of planar four-bar linkages. In Sec. 3, our approach will be presented, which has the benefit of unifying the kinematic analysis codes.

3 A Unified Algorithm for General Four-Bar Motion Analysis

In Ref. [3], we presented a unified equation for the constraint manifolds of all types of planar dyads formed with R and P joints. This transforms the problem of general four-bar motion analysis into that of computing the intersection of two G-manifolds in image space. The latter problem can be readily solved by applying methods developed in the context of computer graphics.

3.1 Dyads and G-Manifolds. Consider three types of dyads, RR, PR, and RP. Their kinematic diagrams are shown in Figs. 3–5.

The design parameters of a RR dyad are fixed pivot coordinates (X_c, Y_c) relative to the fixed frame $\mathbf{F}$, moving pivot coordinates (u, v) relative to the moving frame $\mathbf{M}$ and the length r of the first link. The design parameters of a PR dyad are sliding axis coordinates (L_1, L_2, L_3) of P joint relative to $\mathbf{F}$ and the moving pivot coordinates (u, v) relative to $\mathbf{M}$. The design parameters of an RP dyad are fixed pivot coordinates (X_c, Y_c) relative to $\mathbf{F}$ and sliding axis coordinates (l_1, l_2, l_3) of P joint relative to $\mathbf{M}$.

Let (d_1, d_2) denote the coordinates of the origin of $\mathbf{M}$ with respect to $\mathbf{F}$, and α denote the rotation angle of $\mathbf{M}$ relative to $\mathbf{F}$. Planar quaternion introduces the following mapping from Cartesian space parameters (d_1, d_2, α) to image space coordinates $\mathbf{Z} = (Z_1, Z_2, Z_3, Z_4)$ (see Ref. [8])

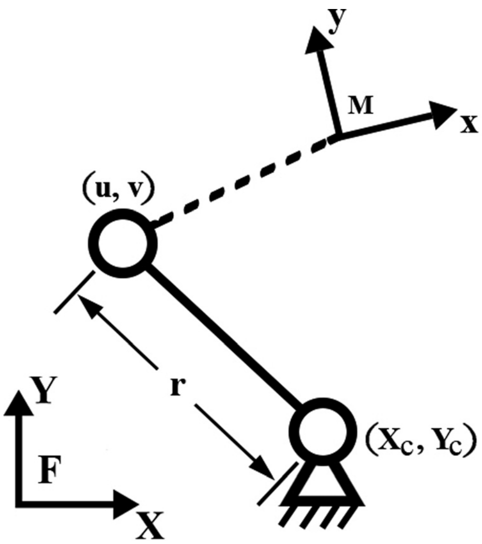

Fig. 3 RR dyad

$$
\begin{aligned}
Z_1 &= (d_1/2)\sin(\alpha/2) - (d_2/2)\cos(\alpha/2) \\
Z_2 &= (d_1/2)\cos(\alpha/2) + (d_2/2)\sin(\alpha/2) \\
Z_3 &= \sin(\alpha/2) \\
Z_4 &= \cos(\alpha/2)
\end{aligned}
\tag{15}
$$

where (Z_1, Z_2, Z_3, Z_4) are homogeneous coordinates of the image space, which is a projective three-space $\mathbb{P}^3(\mathbb{R})$. The inverse relationship from an image point to coordinates in the Cartesian space is

$$
\begin{aligned}
d_1 &= 2(Z_1Z_3 + Z_2Z_4)/(Z_3^2 + Z_4^2) \\
d_2 &= 2(Z_2Z_3 - Z_1Z_4)/(Z_3^2 + Z_4^2) \\
\cos\alpha &= (Z_4^2 - Z_3^2)/(Z_3^2 + Z_4^2) \\
\sin\alpha &= 2Z_3Z_4/(Z_3^2 + Z_4^2)
\end{aligned}
\tag{16}
$$

The two DOF motions of RR-, PR-, and RP-dyads are represented by surfaces called G-manifolds in the image space. Based on Ref. [3], the homogeneous algebraic equation of a G-manifold is given by

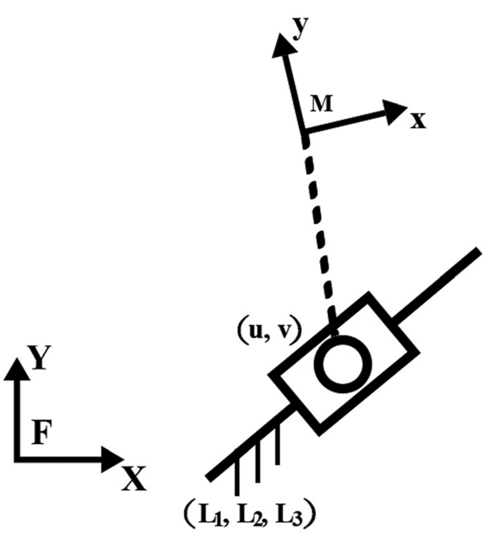

Fig. 4 PR dyad

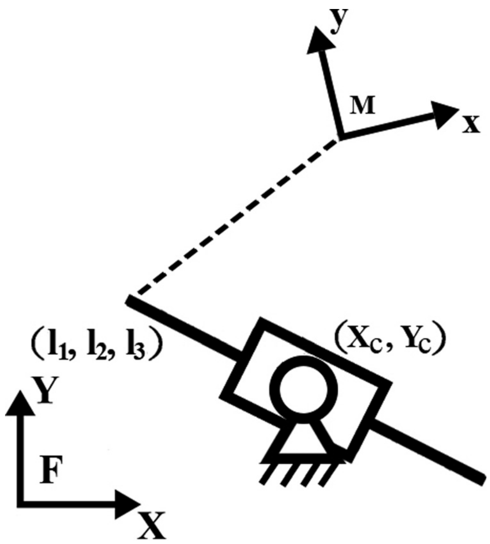

Fig. 5 RP dyad

$$
\begin{aligned}
&q_1(Z_1^2 + Z_2^2) + q_2(Z_1Z_3 - Z_2Z_4) + q_3(Z_2Z_3 + Z_1Z_4) \\
&\quad + q_4(Z_1Z_3 + Z_2Z_4) + q_5(Z_2Z_3 - Z_1Z_4) + q_6Z_3Z_4 \\
&\quad + q_7(Z_3^2 - Z_4^2) + q_8(Z_3^2 + Z_4^2) = 0
\end{aligned}
\tag{17}
$$

with the coefficients, $\mathbf{Q}_G = (q_1, q_2, \ldots, q_8)$, satisfying the following two relations:

$$
\begin{aligned}
q_1q_6 + q_2q_5 - q_3q_4 &= 0 \\
2q_1q_7 - q_2q_4 - q_3q_5 &= 0
\end{aligned}
\tag{18}
$$

Equation (17) represents in general a hyperboloid of one sheet for a RR dyad. It represents a hyperbolic paraboloid I for a PR dyad when $q_1 = q_2 = q_3 = 0$ and a hyperbolic paraboloid II for a RP dyad when $q_1 = q_4 = q_5 = 0$.

Equation (17) can be rewritten in matrix form as $Q_G = \mathbf{Z}^{\mathrm{T}}[G]\mathbf{Z} = 0$, where

$$
[G] = \begin{bmatrix}
q_1 & 0 & \dfrac{q_2+q_4}{2} & \dfrac{q_3-q_5}{2} \\
0 & q_1 & \dfrac{q_3+q_5}{2} & \dfrac{q_4-q_2}{2} \\
\dfrac{q_2+q_4}{2} & \dfrac{q_3+q_5}{2} & q_7+q_8 & \dfrac{q_6}{2} \\
\dfrac{q_3-q_5}{2} & \dfrac{q_4-q_2}{2} & \dfrac{q_6}{2} & q_8-q_7
\end{bmatrix}
\tag{19}
$$

Once a linkage has been synthesized, one can obtain the values of q_i from the original design parameters of its associated dyad (see Ref. [3]). With the intersection algorithm to be presented later on, the parameterization $\mathbf{Z}(t)$ for the intersection curve can be determined, and then the position and orientation of $\mathbf{M}$ can be obtained through Eq. (16). With the $\mathbf{M}$ being calculated at each time instant, those dyad design parameters relative to $\mathbf{M}$, i.e., moving joints or moving lines, can be determined relative to $\mathbf{F}$. Upon working out all the instantaneous information about $\mathbf{M}$ and moving joint or lines, the four-bar motion can then be animated.

3.2 The Intersection Algorithm.

For two G-manifolds $\mathbf{Q}_{G_1}$ and $\mathbf{Q}_{G_2}$, the outline of intersection algorithm is as follows [13]:

(1) Construct the orthonormal transformation matrix $[P]$ which converts $[G_1]$ into diagonal matrix $[\tilde{G}_1]$ by computing the eigenvalues and the normalized eigenvectors of $[G_1]$. The same matrix $[P]$ sends $\mathbf{Q}_{G_1}$ into canonical form $\mathbf{Q}_{\tilde{G}_1}$.

Determine the parameterization $\mathbf{Z}(u, v) = [Z_1(u, v), Z_2(u, v), Z_3(u, v), Z_4(u, v)]$ of the canonical quadric $\mathbf{Q}_{\tilde{G}_1}$.

(2) Compute the matrix $[\tilde{G}_2] = [P]^{\mathrm{T}}[G_2][P]$ for the quadric $\mathbf{Q}_{G_2}$, which transforms $\mathbf{Q}_{G_2}$ into $\mathbf{Q}_{\tilde{G}_2}$. Substitute $\mathbf{Z}(u, v)$ into the algebraic equation of $\mathbf{Q}_{\tilde{G}_2}$, i.e., $\mathbf{Z}^{\mathrm{T}}[\tilde{G}_2]\mathbf{Z} = 0$, to obtain the following equation:

$$\mathbf{Z}(u,v)^{\mathrm{T}}[\tilde{G}_2]\mathbf{Z}(u,v) = a(v)u^2 + b(v)u + c(v) = 0 \quad (20)$$

Then, solve Eq. (20) for u in terms of v and use $\Delta(v) = b^2(v) - 4a(v)c(v) \geq 0$ to determine the domain of v such that real solutions exist for u and we denote the real solutions as $u(v)$. Substitute $u(v)$ into $\mathbf{Z}(u, v)$ to get the parameterization $\mathbf{Z}(v)$ for the intersection of $\mathbf{Q}_{\tilde{G}_1}$ and $\mathbf{Q}_{\tilde{G}_2}$.

(3) Finally, $[P]\mathbf{Z}(v)$ is the parameterization for the intersection of $\mathbf{Q}_{G_1}$ and $\mathbf{Q}_{G_2}$.

During step 1, the canonical form $\mathbf{Q}_{\tilde{G}_1}$ stays the same as

$$aZ_1^2 + bZ_2^2 - cZ_3^2 - dZ_4^2 = 0 \quad (21)$$

regardless of whether $\mathbf{Q}_{G_1}$ is a hyperboloid of one sheet or hyperbolic paraboloid I or hyperbolic paraboloid II. The parameterization $\mathbf{Z}(u, v)$ is given as [13]

$$\mathbf{Z}(u,v) = \left[\frac{u+av}{a}, \frac{uv-b}{b}, \frac{u-av}{\sqrt{ac}}, \frac{uv+b}{\sqrt{bd}}\right] \quad (22)$$

In step 3, $a(v)$, $b(v)$, and $c(v)$ are polynomials of degree at most two in v due to the bilinearity of $\mathbf{Z}(u, v)$. Therefore, $\Delta(v)$ is a polynomial of degree up to four.

Over the course of the algorithm, there is no need to distinguish among the three types of G-manifolds associated with planar RR, PR, and RP dyads, and thereby unifies the analysis of the coupler motion.

4 Examples and Discussions

Now, we present six examples for the planar RRRR, RRRP, RRPR, PRPR, PRRP, and RPPR linkages. For each example, the inputs are two G-manifolds corresponding to two dyads that make up a specific four-bar linkage. The two G-manifolds are represented by their algebraic equations Eq. (17) whose coefficients are given by the vector $\mathbf{Q}_G = (q_1, q_2, \cdots, q_8)$. The output is intersection curve of the two G-manifolds. Since the G-manifolds are represented using homogeneous coordinates (Z_1, Z_2, Z_3, Z_4), for visualization purpose, we project the G-manifold onto the hyperplane $Z_4 = 1$.

4.1 Example: Planar RRRR Linkage. Consider two RR dyads that form a planar RRRR linkage, whose G-manifolds are given by the coefficient vectors

$$\mathbf{Q}_{G_1} = (-2.00, 9.18, 2.68, 2.30, 0.76, 0.41, -5.79, -1.25)$$
$$\mathbf{Q}_{G_2} = (-2.00, 2.48, 0.20, -4.40, -0.20, 0.19, 2.74, -2.43)$$

In this case, both G-manifolds happen to be hyperboloids of one sheet and their curve of intersection has two branches (Fig. 6). Each branch corresponds to one assembly mode of the RRRR linkage. Figure 7 shows the two assembly modes of the linkage as well as two sets of coupler positions corresponding to the two branches.

4.2 Example: Planar RRRP Linkage. Consider an example for RRRP (crank–slider) mechanism, whose G-manifolds are given by the coefficient vectors

$$\mathbf{Q}_{G_1} = (-2.00, -4.00, -6.00, 0, 2.00, -4.00, 3.00, -6.50)$$
$$\mathbf{Q}_{G_2} = (0, 0, 0, 2.00, 4.00, 10.00, 5.00, 1.00)$$

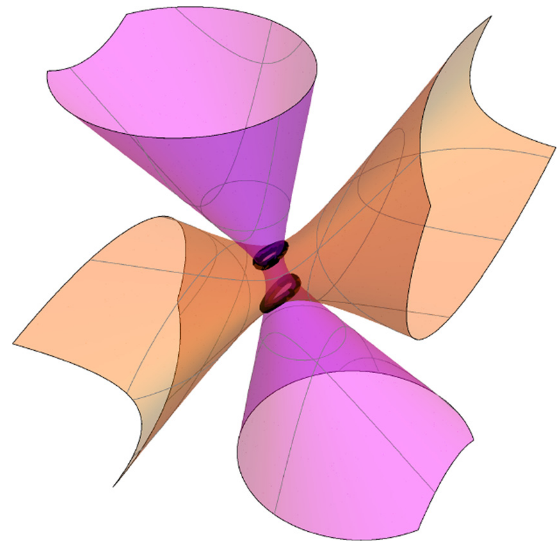

Fig. 6 The image curve of a RRRR linkage as intersection of two G-manifolds

The G-manifolds and their intersection curve are shown in Fig. 8. One G-manifold is hyperboloid of one sheet and the other one hyperbolic paraboloid I. In this case, the curve of intersection has also two branches and each corresponds to one assembly mode of a crank–slider mechanism. Two sets of coupler positions corresponding to the two branches and the associated assembly modes of the mechanism are shown in Fig. 9.

4.3 Example: Planar RRPR Linkage. Consider an example for RRPR (swing–block) mechanism, whose G-manifolds are given by the coefficient vectors

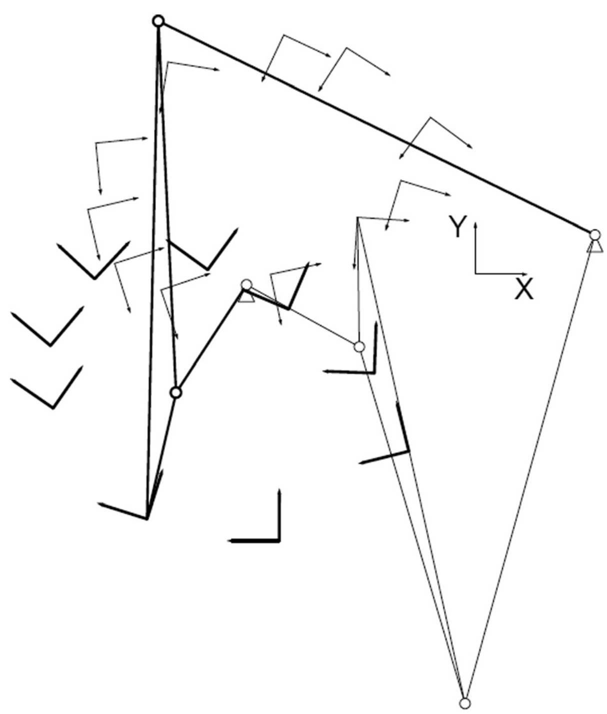

Fig. 7 Two assembly modes of a RRRR linkage with their corresponding coupler positions are shown in thick and thin lines, respectively

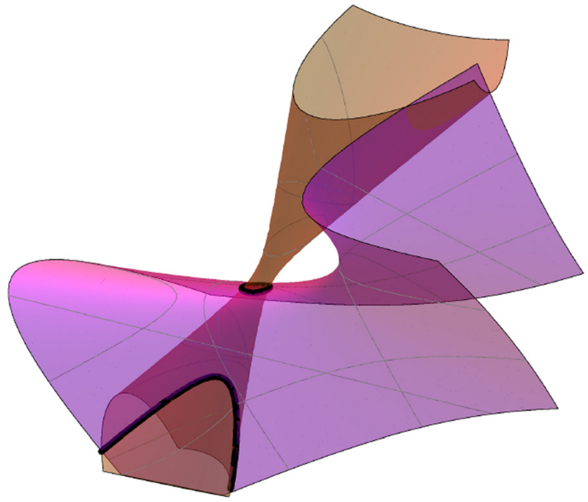

Fig. 8 The image curve of a RRRP linkage as intersection of two G-manifolds

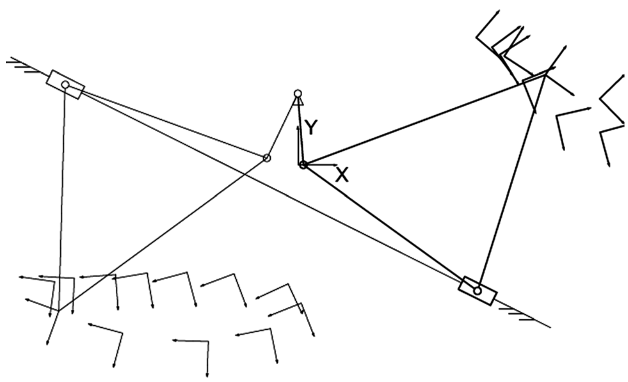

Fig. 9 Two assembly modes of a RRRP linkage with their corresponding coupler positions are shown in thick and thin lines, respectively

$$\mathbf{Q}_{G_1} = (-2.00, -4.00, -5.98, 0, 2.00, -4.00, 2.99, -4.97)$$
$$\mathbf{Q}_{G_2} = (0, 0, 2.00, 0, 0, -4.00, -3.00, 3.00)$$

The G-manifolds and their intersection curve are shown in Fig. 10. One G-manifold is hyperboloid of one sheet and the other one

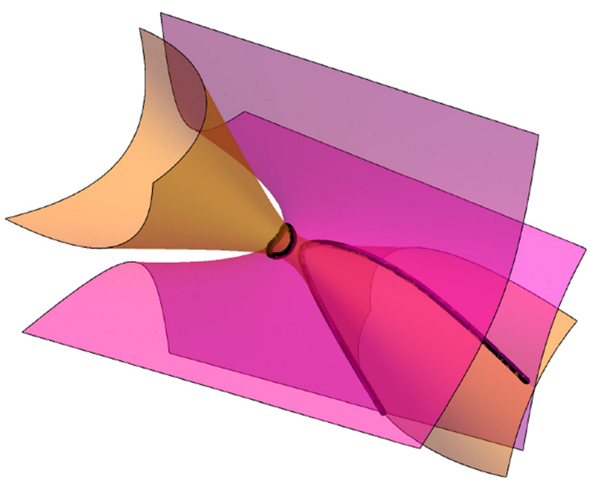

Fig. 10 The image curve of a RRPR linkage as intersection of two G-manifolds

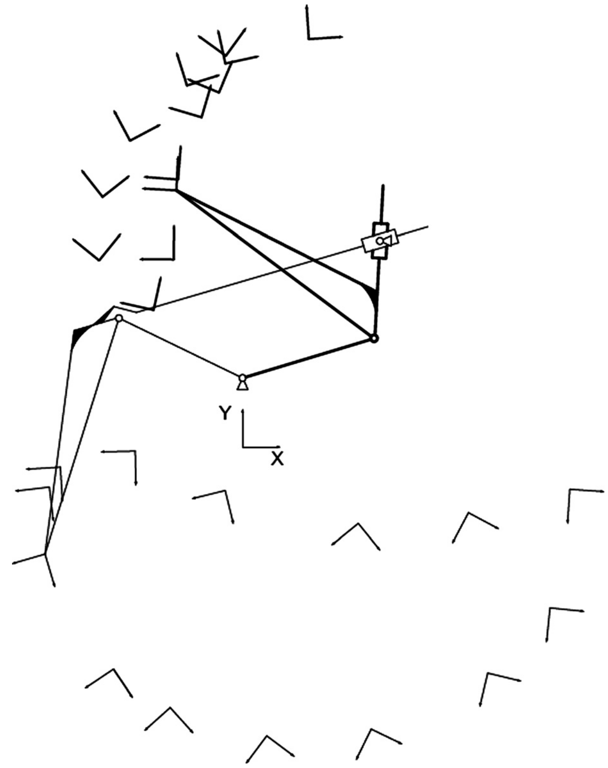

Fig. 11 Two assembly modes of a RRPR mechanism with their corresponding coupler positions are shown in thick and thin lines, respectively

hyperbolic paraboloid II. There are two branches of the intersection curve and each corresponds to one assembly mode of a swing–block mechanism. Two sets of coupler positions corresponding to the two branches and the associated assembly modes of the mechanism are shown in Fig. 11.

4.4 Example: Planar PRPR Linkage. Consider an example for PRPR (slider–swinging block) mechanism, whose G-manifolds are given by the coefficient vectors.

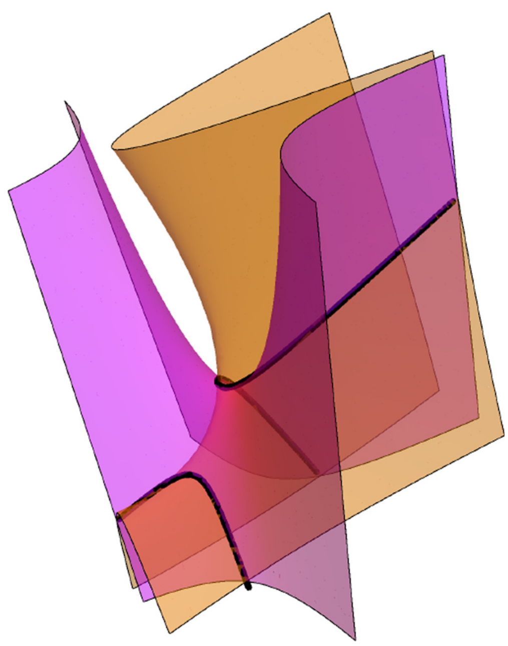

Fig. 12 The image curve of a PRPR linkage as intersection of two G-manifolds

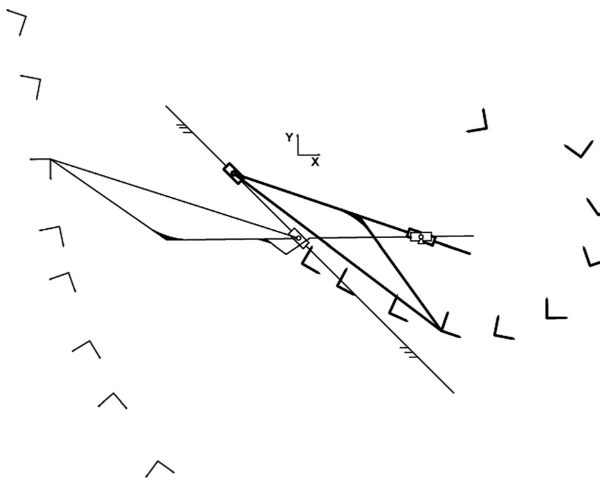

Fig. 13 Two assembly modes of a PRPR linkage with their corresponding coupler positions are shown in thick and thin lines, respectively

$$\mathbf{Q}_{G_1} = (0, 0, 0, 2.00, 2.00, -16.00, 4.00, 2.00)$$
$$\mathbf{Q}_{G_2} = (0, 0, 2.00, 0, 0, -6.00, 2.00, -2.00)$$

The G-manifolds and their intersection curve are shown in Fig. 12. One G-manifold is hyperbolic paraboloid I and the other one hyperbolic paraboloid II. There are two branches for the intersection curve and each corresponds to an assembly mode of slider–swinging block mechanism. Two sets of coupler positions corresponding to the two branches and the associated assembly modes of the mechanism are shown in Fig. 13.

4.5 Example: Planar PRRP Linkage. Consider an example for PRRP (double-slider) mechanism, whose G-manifolds are given by the coefficient vectors

$$\mathbf{Q}_{G_1} = (0, 0, 0, 1.86, -0.73, -5.84, 3.08, 0.57)$$
$$\mathbf{Q}_{G_2} = (0, 0, 0, 1.86, 0.74, -10.96, 3.44, 1.30)$$

Both G-manifolds are hyperbolic paraboloid I, and their intersection curve is shown in Fig. 14. There is only one intersection curve corresponding to the single assembly mode of a double-slider mechanism. The PRRP linkage together with the coupler motion is shown in Fig. 15.

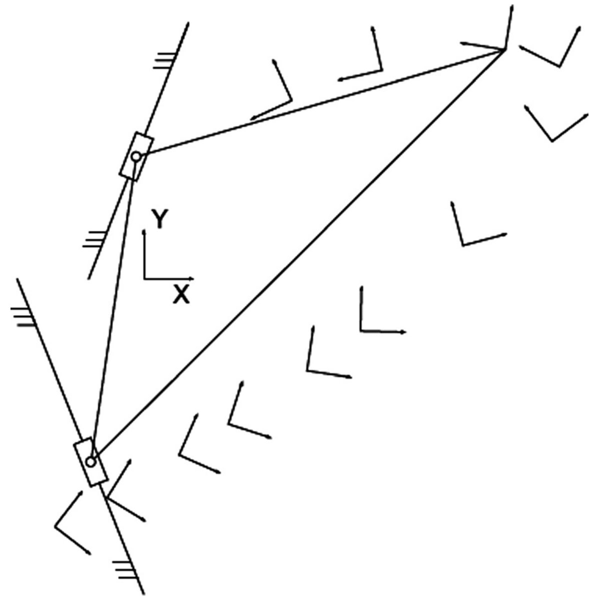

Fig. 15 A PRRP linkage with their corresponding coupler positions

4.6 Example: Planar RPPR Linkage. Consider an example for RPPR (double-swinging block) mechanism, whose G-manifolds are given by the coefficient vectors

$$\mathbf{Q}_{G_1} = (0, 0.47, 1.94, 0, 0, 0.50, -0.02, 4.08)$$
$$\mathbf{Q}_{G_2} = (0, 1.86, -0.74, 6.00, 0, 3.46, -3.77, 4.20)$$

The G-manifolds and their intersection curve are shown in Fig. 16. Both G-manifolds are hyperbolic paraboloid II. The intersection curve has only one branch which corresponds to a double-swinging block mechanism. The RPPR linkage together with the coupler positions is shown in Fig. 17.

5 Conclusions

In this paper, we present a unified algorithm to the analysis and simulation of all types of planar four-bar motions. Instead of taking the approach of loop-closure equation toward simulations of different four-bar types, we employ planar quaternion to map a

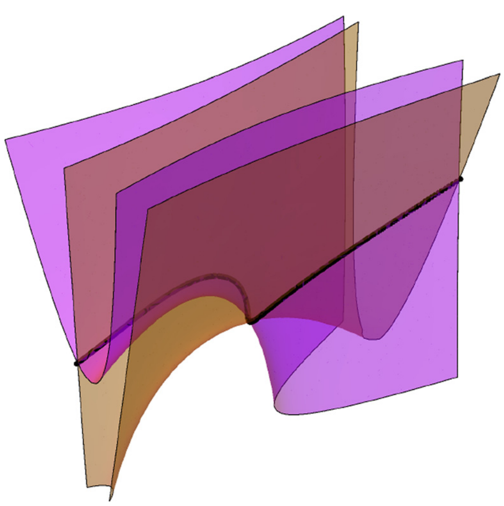

Fig. 14 The image curve of a PRRP linkage as intersection of two G-manifolds

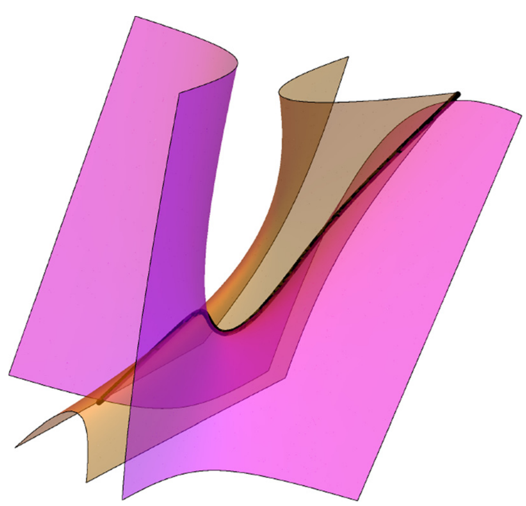

Fig. 16 The image curve of a RPPR linkage as intersection of two G-manifolds

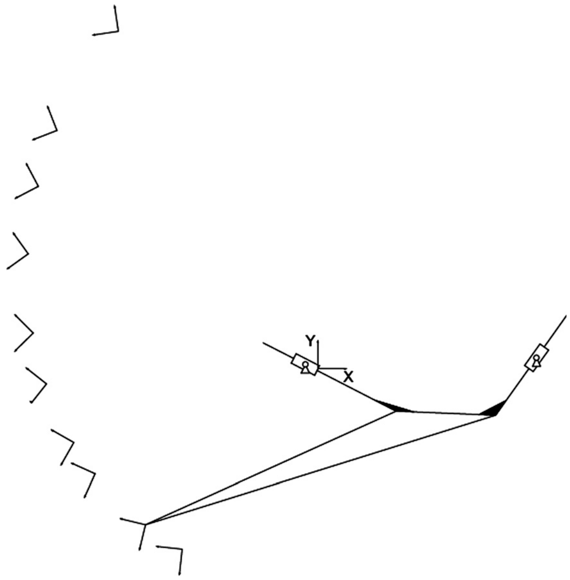

Fig. 17 A RPPR linkage with its coupler positions

four-bar mechanism into a pair of G-manifold in image space and therefore the four-bar coupler motion ends up being the intersection curve. The animation problem is then reduced to the problem of determining the parameterization for the intersection curve. Since our G-manifolds are in the category of quadrics, and limited to hyperboloid of one sheet and hyperbolic paraboloid, there exists a simple and efficient algorithm to find the parameterization. The six examples provided fully demonstrate the effectiveness of this algorithm.

Acknowledgment

The work has been supported by National Science Foundation under Collaborative Research grant to Stony Brook University (Q. J. Ge, Grant No. CMMI-0856594).

References

[1] Erdman, A., and Sandor, G., 2001, *Mechanism Design: Analysis and Synthesis*, 4th ed., Prentice Hall, Upper Saddle River, NJ.
[2] Norton, R. L., 2012, *Design of Machinery: An Introduction to the Synthesis and Analysis of Mechanisms and Machines*, 5th ed., McGraw-Hill, New York.
[3] Ge, Q. J., Zhao, P., and Purwar, A., 2013, "A Task Driven Approach to Unified Synthesis of Planar Four-Bar Linkages Using Algebraic Fitting of a Pencil of G-Manifolds," ASME Paper No. DETC2013-12977.
[4] SyMech, 2014, SYMECH, SyMech Inc., San Francisco, CA, http://www.symech.com
[5] Heron, 2014, WATT, Heron Technologies b.v., Reefalf, The Netherlands, http://www.heron-technologies.com/watt
[6] Artas, 2014, SAM, Artas Engineering Software, Het Puyven, The Netherlands, http://www.artas.nl
[7] MSC, 2014, ADAMS, MSC Software Corp., Newport Beach, CA, http://www.mscsoftware.com/product/adams
[8] Bottema, O., and Roth, B., 1979, *Theoretical Kinematics*, North Holland, Amsterdam, The Netherlands.
[9] McCarthy, J. M., 1990, *Introduction to Theoretical Kinematic*s, MIT, Cambridge, MA.
[10] Ravani, B., and Roth, B., 1984, "Mappings of Spatial Kinematics," ASME J. Mech. Des., **106**(3), pp. 341–347.
[11] Levin, J., 1976, "A Parametric Algorithm for Drawing Pictures of Solid Objects Composed of Quadric Surfaces," Commun. ACM, **19**(10), pp. 555–563.
[12] Levin, J., 1979, "Mathematical Models for Determining the Intersections of Quadric Surfaces," Comput. Graphics Image Process., **11**(1), pp. 73–87.
[13] Dupont, L., Lazard, D., Lazard, S., and Petitjean, S., 2008,"Near-Optimal Parameterization of the Intersection of Quadrics: I. The Generic Algorithm, II. A Classification of Pencils and III. Parameterizing Singular Intersections," J. Symb. Comput., **43**(3), pp. 168–232.
[14] Wu, J., Ge, Q. J., Gao, F., and Guo, W. Z., 2011, "On the Extension of a Fourier Descriptor Based Method for Four-Bar Linkage Synthesis for the Generation of Open and Closed Paths," ASME J. Mech. Rob., **3**(3), p. 031002.